ELSEVIER

Journal of Photochemistry and Photobiology A: Chemistry 111 (1997) 253–263

Journal of PHOTOCHEMISTRY AND PHOTOBIOLOGY A: CHEMISTRY

Chemical(photo-activated) coupled biological homogeneous degradation of *p*-nitro-*o*-toluene-sulfonic acid in a flow reactor

J. Bandara [a], C. Pulgarin [b,*], P. Peringer [b], J. Kiwi [a,*]

[a] *Institute of Physical Chemistry, Swiss Federal Institute of Technology (EPFL), 1015 Lausanne, Switzerland*

[b] *Institute of Environmental Engineering, Bioengineering, Swiss Federal Institute of Technology (EPFL), 1015 Lausanne, Switzerland*

Received in revised form 8 August 1997

Abstract

This study presents the combined photochemical (Fenton) and biological flow reactor degradation of *p*-nitrotoluene-*ortho*-sulfonic acid (*p*-NTS). *p*-NTS is a compound whose degradation is not possible by waste water bacteria. From this point of view it is considered as a non-biodegradable intermediate found in the manufacture of dyes, surfactants and brighteners. By way of HPLC technique it is shown that the photochemical pretreatment of *p*-NTS induces dearomatization due to ·OH radical attack. A concomitant 20–25% decrease in the initial carbon content during the photochemical pretreatment was observed along the abatement of the aromaticity. This study shows that the intermediates produced in the pretreatment stage are biodegradable. After pretreatment a minimum residual H_2O_2 ($<0.2\ mg\ l^{-1}$) was attained. This level of oxidant did not interfere with the subsequent biological degradation. The influence of the reaction parameters such as: input concentration of *p*-NTS, rate of H_2O_2 addition, reactor flow rate, TOC reduction rate and BOD_5/COD as a function of the time of photochemical pretreatment are reported. At a flow rate of $0.18\ l\ h^{-1}$ (5.5 h residence time) a photochemical degradation efficiency of 75%, a biological degradation efficiency of 52% and an overall degradation efficiency for the coupled process of 88% was observed. The disappearance of *p*-NTS in the photochemical reactor, the growth and degradation of the benzoquinone like aromatic intermediate followed by the appearance short chain aliphatic compounds are reported as a function of pretreatment time.The increase in BOD/TOC as function of pretreatment time has been correlated to the *p*-NTS and aliphatic recalcitrants existing in the solution. The biological degradation was observed to be strongly dependent on the flow used and on the pollutant loading of the solution. These were the two main parameters affecting the degradation in the bioreactor.

Keywords: Coupled flow reactors; Photochemical pretreatment; Fenton systems; *p*-Nitro-*ortho*-toluene-sulfonate

1. Introduction

Chemical pretreatment methods are necessary to destroy recalcitrant organic compounds in water. Since pretreatment methods are in general expensive they should be coupled with the much cheaper biological degradation as soon as the toxicity of the initial persistent pollutant is no more present [1]. During the last years coupled treatment technologies have shown to be more economical and therefore more applicable to complex waste problems than stand-alone advanced oxidation. This study presents an example of coupling advanced oxidation pretreatment with biotreatment.

An initial oxidation of organic compounds by ·OH radicals generated in situ has been shown to react quickly and non-selectively with many aromatics by way of the photo-assisted Fenton reaction [2]. A non-biodegradable compound *p*-NTS has been chosen due to: (a) it has nitro- and sulfate groups as electron withdrawing groups conferring non-biodegradability to the molecule; (b) its presence in effluents from the Swiss chemical industry; (c) previous work out of our laboratory reporting its relatively slow abatement via TiO_2/H_2O_2 in batch reactions [3] preliminary work indicated promising results for *p*-NTS degradation [4]. The pretreatment will be shown to allow the subsequent biological treatment to proceed and to achieve high overall abatement efficiency.

Few studies and not much engineering work has been devoted until now to the coupling of chemical and biological flow reactors useful in removing pollutant in solution [5–7]. The present study focus on the photochemical–biological coupled degradation of *p*-NTS in solution. The shortest residence time possible in the first stage is sought since photons are used in the first stage with the consequently high electricity cost. The coupled flow reactor is shown below in Fig. 1.

* Corresponding authors.

1010-6030/97/$17.00
PII S1010-6030(97)00249-9

It was designed to test for different flow rates, organic loads, recirculation rates, rate of oxidant addition and other operational parameters. The most effective reduction of the total organic carbon (TOC) of the *p*-NTS in the combined reactor was sought during this study by suitable combination of the parameters mentioned above. One of the problems encountered during this work was the adjustment of the experimental variables to use up completely the H_2O_2 in the photoreactor. In this way, the detrimental action of the oxidant is avoided on the biological stage (bioreactor). This study led to the design and construction of combined reactor that would: (a) treat waste-waters in situ up to an effluent 4 m^3 m^{-3} reactor/day; (b) have a small volume with respect to the volume of a reactor using suspended biomass in the second stage; and (c) stay operational for long periods in spite of changes in the load charge (concentration), pH, salinity and flow.

2. Experimental

2.1. Photoreactor

Annular geometry has been employed in the photochemical reactor as shown in Fig. 1. The glass spiral in the photochemical reactor is about 20 m long and 8 mm in diameter. The lamp is positioned in such a way that its center line passes through the focal axis of the coil reactor. The lamp used was a 400 W medium pressure Hg-lamp 40 cm long (applied photophysics) with a photon total output of 5×10^{19} s^{-1}. The predominant radiation λ was observed at 366 nm with 50% of the Hg lamp output (equivalent to ~ 15 W). Care has been taken that all photons are absorbed in the optical thickness of the reactor coil since the scattering effects are less significant in a reacting medium having high optical absorption. The reactor mixing flask had a volume of 1 l. The runs were carried out at room temperature. The *p*-NTS solution was fed into the system from a 18 l reservoir and the H_2O_2 was added by means of a peristaltic pump into the 1 l mixing flask as shown in Fig. 1.

2.2. Bioreactor

The fixed bed laboratory reactor (FBLR) consisted of a column containing biolite in a 2-l feeding reactor (Bioengineering, Switzerland). The pH, temperature and O_2 flow were controlled and adjusted at 7.0, 24°C and 6.5 mg O_2 l^{-1}, respectively. The aeration was about 150 l h^{-1} and the agitation speed 1200 rpm. The medium volume in the column was about 1.2 l. The effluent of the photochemical stage was circulated by a peristaltic pump (Watson Marlow) through the bottom of the column, which operated as an up-flow reactor. The recirculation flow was fixed in each case depending on the specific degradation efficiency aimed at. The flow of air and the pH were measured at the bottom and at the top of the column. At the recirculating rates worked, excellent contact between the effluent and the immobilized biomass was attained in the bioreactor. Other details for the second biological stage have been reported elsewhere [8,9].

2.3. Materials and procedures

p-NTS was a gift from Ciba (Monthey). $FeCl_3 \cdot 6H_2O$ and H_2O_2 were Fluka (30% w/w) analysis grade (p.a.) and have been used without further purification. In the biological reactor the nutrient salts used (P, N, K and oligoelements) were added from standard solutions during biological degradation

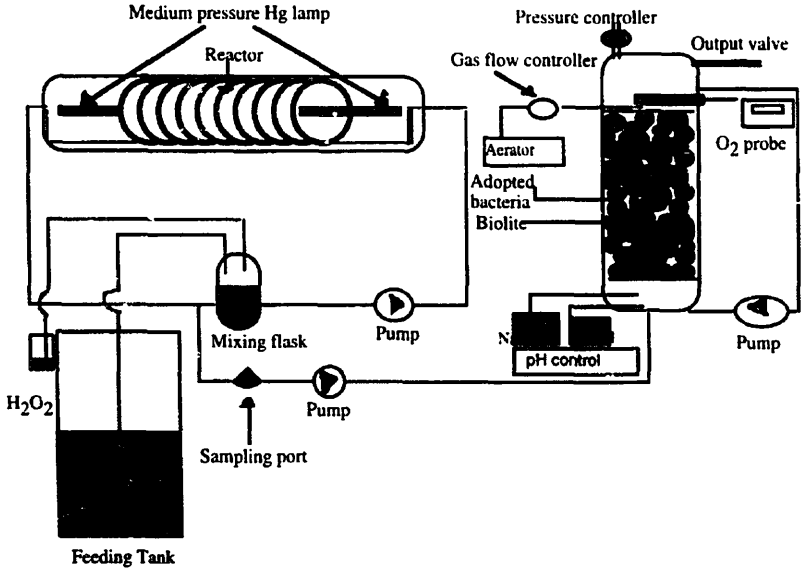

Fig. 1. Schematic of the photochemical-biological combined reactor used throughout this work. For other details see text.

[4,8,9]. The mixture of these nutrients with the exception of phosphate salts were added in the 18 l feeding tank. Phosphate was added separately to the NaOH vessel positioned immediately before the bioreactor. Phosphate (PO_4^{3-}) was observed to inhibit the degradation in the photoreactor slowing down H_2O_2 decomposition.

The consumption of H_2O_2 during the reaction was followed by the Merckoquant® test for peroxides. The peroxydase adsorbed in the analysis paper transfers the oxygen of the peroxide to an organic dye that is blue in color. The blue shade of the oxidized form of the dye is in proportion to the peroxide concentration in solution up to 25 mg l^{-1}. An extremely low residual H_2O_2 level from the first stage was detected in this way at the junction between the two stages in the flow reactor. It was never allowed to exceed 0.2 mg $H_2O_2\,l^{-1}$.

2.4. Analysis in solution

Total organic carbon (TOC) was monitored during this study via a Shimadzu 500 instrument provided with an automatic auto-sampler. High-pressure liquid chromatography (HPLC) was carried out via a Varian 9100 LC unit equipped with a 9065 diode array. The column used was Spherisorb ODS-2 5 μm and the mobile phase consisted of a solution Na-acetate in acetonitrile–water solution. This allows to measure the *p*-NTS concentration in solution. It also allows to follow the formation and decay kinetics of the aromatic and the aliphatic compounds during the process. Spectrophotometric measurements were performed via Hewlett-Packard 386/20 N diode array. Proton nuclear magnetic resonance (NMR) was carried out by means of a Brucker ACP-2000 apparatus to observe the disappearance of the aromatic compounds and the appearance of the aliphatic intermediates in the solution during the degradation. Chemical oxygen demand (COD) was carried out via a Hach-2000 spectrophotometer using dichromate solution as the oxidant in strong acid media. The inorganic ions in the solution were followed in a Dionex ion-liquid chromatograph provided with an IonPac® anion type AS4 column.

2.5. Test of bacterial activity

Biological oxygen demand (BOD) was carried out by means of a Hg free WTW 2000 Oxytop unit thermostated at 20°C. The Zahn–Wellens test was used with high bacterial concentration of 1 g l^{-1} [3,4]. The sludge from the Lausanne STEP station was aerated for a 24 h period and subsequently centrifuged. Redissolution of the centrifugated portion was then diluted to 1 g l^{-1} and used in the Zahn–Wellens test. Toxicity during the photochemical pretreatment was assessed using the Microtox® technique. The bioluminescence of *Photobacterium phosphoreum* in the presence of *p*-NTS was followed as a function of photochemical pretreatment time [3].

3. Results and discussions

3.1. Photochemical pretreatment of p-NTS in the reactor. Batch system operation

Fig. 1 presents a schematic view of the coupled photochemical–biological flow reactor used during this study. The left half shows the photochemical pretreatment unit (reactor) and the right hand side the scheme of the bioreactor. Preliminary experiments carried out at pH 2.7 show that the amount of H_2O_2 added to the feeding tank (18 l) has a significant influence on the rate of the degradation of a concentrated *p*-NTS solution, as shown in Fig. 2a. A flow rate of 0.8 ml 18 l^{-1} equals 13.3 mg l^{-1} based on 30% H_2O_2 purity. The recirculation rate used in the photoreactor was 500 ml min^{-1} (30 l h^{-1}). The TOC measured reflects the amount of *p*-NTS transformed into CO_2 during the pretreatment. The rate of TOC decrease in the solution was seen to become bigger with the amount of added H_2O_2 (Fig. 2a). Similar observations have been reported previously reported [7,8]. Fig. 2a shows that the degradation of an initial solution containing 0.104 moles of *p*-NTS 18 l^{-1}. Within 16 h the oxidation of *p*-NTS is almost complete and trace (Fig. 2d) indicates that 144 ml H_2O_2 is consumed during this period equivalent to 1.41 moles H_2O_2. This is an oxidant to pollutant molar ratio of 13.5:1. This experimental result allows to suggest the pretreatment stoichiometry as:

$$C_7H_7O_5NS + 13\,H_2O_2 + 19/2\,O_2 \rightarrow 7\,CO_2 + 29/2\,H_2O + HNO_3 + H_2SO_4 \quad (1)$$

The addition of H_2O_2 was made more accurate when H_2O_2 was added into the smaller mixing flask (1 l) as shown in Fig. 1. The degradation results of *p*-NTS after 1 h under a better control of the oxidant to substrate ratio is shown in Fig. 2b. This setup allowed accurate monitoring of the reagents added during the degradation process.

The spectrum of the solution used in Fig. 2a,b and the light penetration in the reactor coil play an important role during the *p*-NTS degradation. The solution used had an absorbance close to 3.0 at $\lambda = 366$ nm for an optical pathlength of $d = 0.8$ cm equivalent to the coil diameter. The degradation rate reported in Fig. 2a,b proceeds at a considerable higher rate when photo-Fenton pretreatment was used than when an supported TiO_2/H_2O_2 was used during the catalyst pretreatment. Moreover Fe^{3+}-ions remain in solution during the whole operation and no fouling was observed on the reactor walls up to 1 month reactor operation. Heterogeneous pretreatment was carried out by TiO_2 supported on glass beds or quartz wool. Since light penetration is only in the micron range on the TiO_2-beads, this seems to affect adversely the efficiency of the pretreatment [10].

During photochemical pretreatment it was intended to: (a) have a short pretreatment time which avoids long irradiation periods with the 400 W Hg-lamp and consequently the high cost of the electricity used. This represents about 60% of the total operational costs of photochemical reactors [4,11]. The

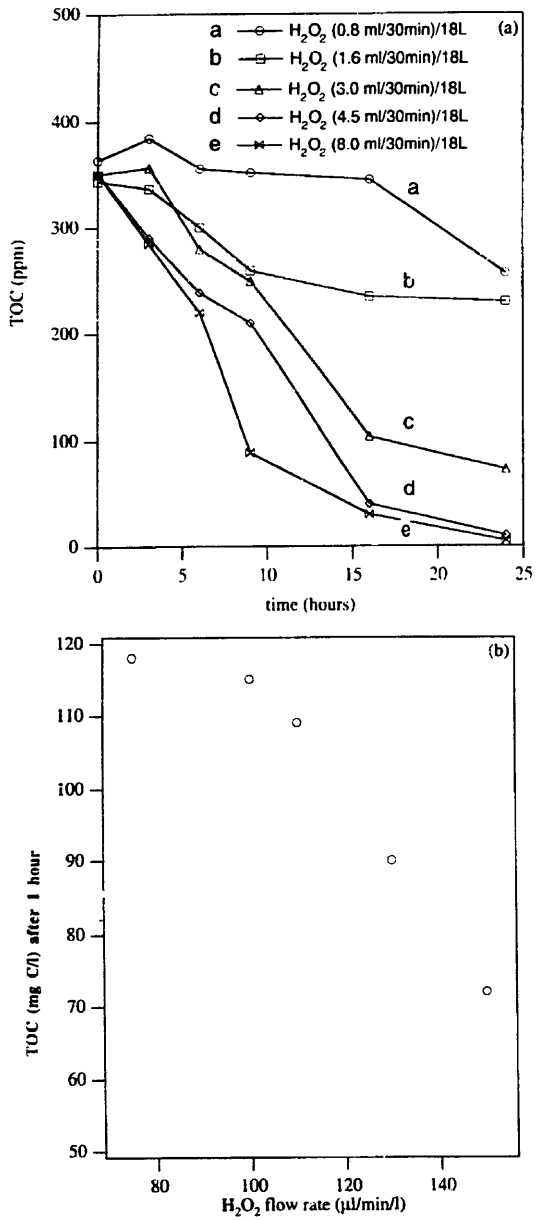

Fig. 2. (a) Effect of the rate of oxidant addition in the feeding tank on the total organic carbon (TOC) decrease as a function of time for a solution containing *p*-NTS ($4.2.8\times10^{-3}$ M) and $FeCl_3$ (0.8×10^{-3} M) at pH 2.7. (b) Final TOC after 1 h photoreactor pretreatment as a function of oxidant flow rate added into mixing flask for the same solution as used in Fig. 2a.

signal at ~5 ppm represent the signals of the residual protons in the deuterated sample; (b) have a suitable combination of concentration, flow rate, recirculation and dilution rate allowing to attain a TOC level of 118 ppm carbon with 80 µl min^{-1} l^{-1} H_2O_2 flow rate within 1 h (Fig. 2b). This carbon level is suitable to feed the bacteria in the bioreactor and sustain their activity at a convenient conversion rate; (c) reduce 50–65% the initial carbon content in the solution. This amount was shown to be sufficient to eliminate the aromatic compounds formed during *p*-NTS degradation in the photoreactor (see below NMR results in Fig. 3); (d) find a flow rate common to both reactors allowing a convenient degradation and dilution rate during reactor operation; and finally (e) consume all the H_2O_2 of the first stage. Due to its known bactericide character any H_2O_2 left over in the first stage would hinder the functioning of the biological stage and has to eliminated during the pretreatment period.

3.2. Chemical and biological characteristic of photochemically pretreated p-NTS solutions

Fig. 3 shows the reduction in aromaticity via ^1H NMR technique. In Fig. 3a,b,c the signal reduction is recorded for a *p*-NTS solution (4.2×10^{-3} M) where Fe^{3+} (0.8×10^{-3} M) has been added along of H_2O_2 (4.5 ml 30 min^{-1} 18 l^{-1}) and irradiated with a Hg source as reported previously in Fig. 2a. Subsequently the solutions (Fig. 3a,b,c) are dried at 40°C in a crystallyzer for two days and the residual deposit is mixed with D_2O. The signal at ~5 ppm represent the signals of the residual protons in the deuterated sample since a small residual humidity could never be eliminated on the samples to be analyzed.

Fig. 3a shows the signals for the aromatic protons between 7.5 and 8.5 ppm and for methyl groups at 2.7 ppm. Fig. 3b shows that the signals associated with the spectra of the aromatic protons have decreased significantly after 15 min reaction. Notice that the sensitivity of the scale used in this measurement is increased by a factor of three with respect to Fig. 3a. This is interpreted as non-destructive modification occurring in the aromatic cycle due to the Fenton induced hydroxylation [3,4,7,8]. Aliphatic species appear as degradation products showing signals between 2 and 2.7 ppm. Spectrum (c) shows that after 30 min irradiation the practically no aromatic protons are present. Notice in Fig. 3c that a widely expanded scale has been used with a sensitivity five times higher as in Fig. 3a. Concomitantly, the signals of aliphatic species with electron withdrawing character groups (1.2–4.2 ppm) become more abundant as well as a second class of aliphatic compounds at 3.9–4.0 ppm. The decrease in the aromatic products was seen to occur in less than 1 h.

The ratio COD to TOC for a solution is shown in Fig. 4a as a function of pretreatment time up to 60 min. The COD measurements have been taken after careful checking that no residual H_2O_2 is available in solution after initial pretreatment. The solution used comes from an 18 l feeding tank since this experiment involves a continuous type flow process. The ratio of the chemical oxygen demand COD/TOC was seen to decrease with pretreatment time since more oxidized intermediates become available per milligram C in solution. A low ratio for COD/TOC is attained after 20 min pretreatment in Fig. 4a. The average oxidation state for the

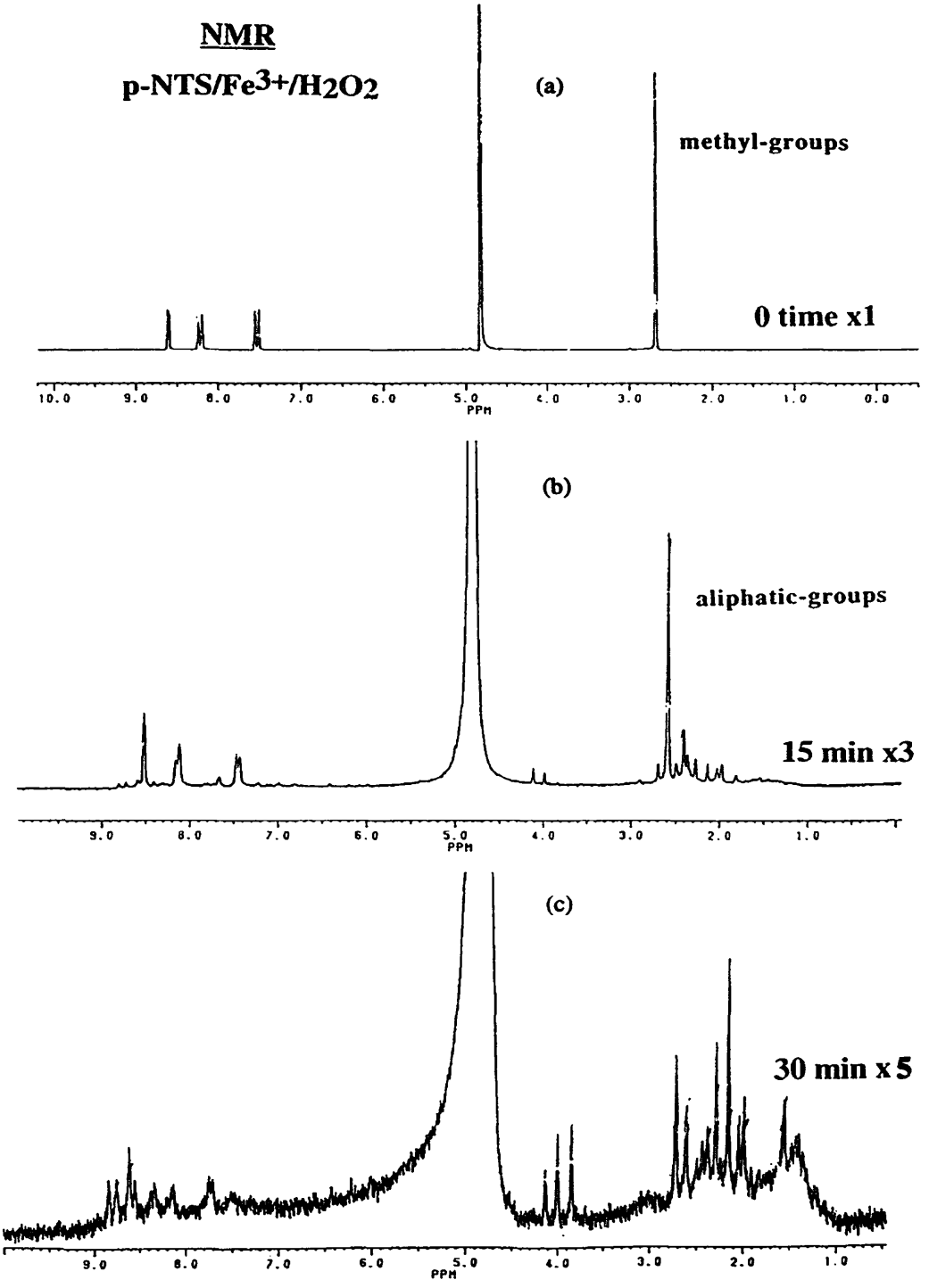

Fig. 3. ^{1}H NMR spectroscopy of *p*-NTS as a function of irradiation times for a solution with the same make up as used in Fig. 2.

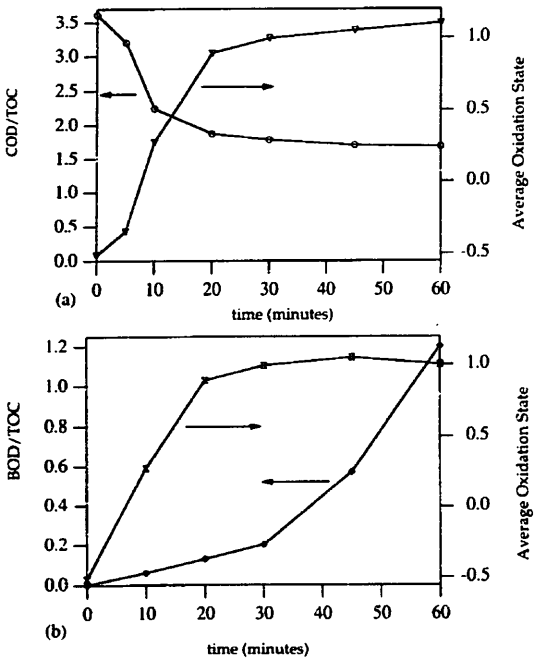

Fig. 4. (a) Ratio of chemical oxygen demand (COD) and total organic carbon (TOC) as a function of pretreatment time of a solution like used in Fig. 2a. (b) Ratio of biological oxygen (BOD_5) demand and pretreatment time for the solution used in Fig. 4a. The average oxidation state is shown in each case.

The BOD_5/TOC ratio represents the amount of O_2 consumed in 5 days per gram of C present in the solution. The ratio BOD_5/TOC for the solution used in Fig. 4a is shown in Fig. 4b (left hand side axis). The corresponding average oxidation state is shown in the right hand side axis. The initial BOD_5/TOC was zero as expected. The BOD_5 values found were: 70 (30 min, 300 mg C l^{-1}; 125 (45 min, 225 mg C l^{-1}) and 165 (60 min, 150 mg C l^{-1}). The BOD_5/TOC ratio is seen to increase with pretreatment time. Beyond 20 min it was seen to attain a relatively high value. This suggest that only when the *p*-NTS and the initial aromatic intermediate compounds have been removed from solution the BOD_5 drastically increases. The ratio BOD_5/TOC of 0.45 (Fig. 4b) shows that above 40 min the intermediates present in the solution are in highly oxidized state.

Fig. 5 shows the effect of the first stage pretreatment time for a solution as used Fig. 2a (trace d) on the ratio BOD_5/COD. The beneficial effect of the photo-treatment on the biodegradability of *p*-NTS is readily seen. The chemical oxidation by the photo-assisted Fenton system generates intermediates with more oxidized functional groups in agreement with earlier reports involving Fenton oxidation of common pollutants [1,2,12]. After 30 min the ratio BOD_5/COD is seen to be >0.4. This means that after this short time the *p*-NTS reaches the biodegradability index for truly biodegradable waste-waters. Pretreatment times of 30 min and beyond in Fig. 5 suggest that when *p*-NTS is almost removed from the system the values for BOD_5 markedly increase.

intermediates is shown in right hand side axis and is a function of pretreatment time. These values have been estimated according to Ref. [1]:

$$\text{Average Oxidation State} = \frac{4(\text{TOC} - \text{COD})}{\text{TOC}} \qquad (2)$$

where TOC is expressed in moles of C l^{-1} and COD is in moles of O_2 l^{-1}.

Eq. (2) has been used to relate the average chemical oxidation state with the biodegradability of the organic compounds in solution. A plateau is observed for the COD/TOC ratio after 20 min in Fig. 4. A priori this suggests that the chemical nature of these intermediates do not vary significantly after 20 min reaction. But such a statement would contradict the results reported in Fig. 4b, where it is shown that the BOD data increases drastically between 20 and 60 min. Two processes could be suggested as taking place in Fig. 4a.

$$p\text{-NTS} \xrightarrow{k_1} [\text{aromatic oxidized intermediates}]$$
$$+ CO_2 \xrightarrow{k_2} [\text{aliphatic oxidized intermediates}] \qquad (3)$$
$$+ CO_2 \xrightarrow{k_3} CO_2$$

where $k_1 > k_2 \gg k_3$.

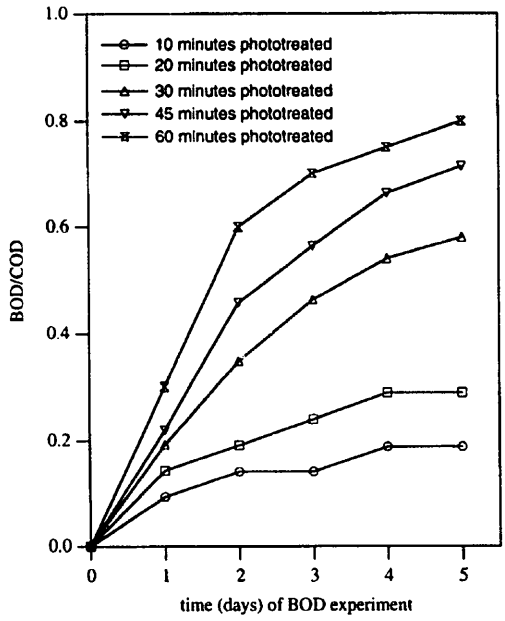

Fig. 5. Ratio of biological oxygen demand (BOD_5) and chemical oxygen demand (COD) as a function of pretreatment time as indicated in the captions in Fig. 5.

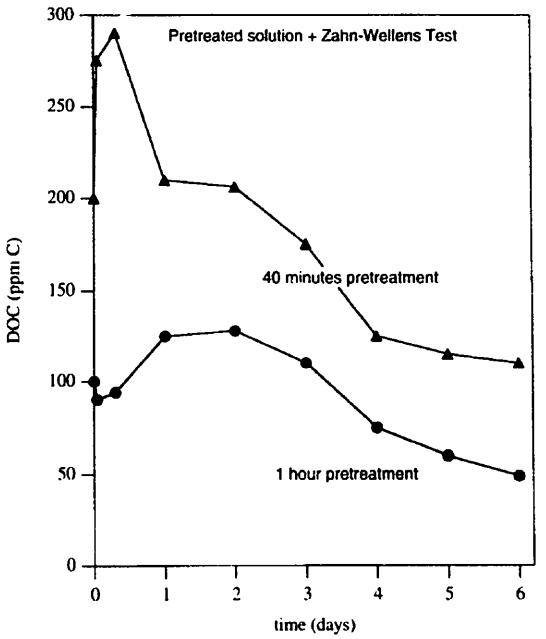

Fig. 6. Dissolved organic carbon (DOC) as a function of time using the biological Zahn–Wellens test as a function of two different pretreatment times. The solution used was the same as Fig. 2a.

This is in agreement with the results shown previously in Fig. 4a,b.

The effect of the time of photochemical dearomatization on the biodegradability of *p*-NTS was carried out by means of the Zahn–Wellens test [13]. The biodegradation was measured following the decrease in the dissolved organic carbon (DOC) as a function of time. This is shown in Fig. 6. This test was used to follow the evolution of the dissolved organic carbon (DOC) after photochemical pretreatment. This test resembles the conditions found in the aerobic waste water treatment of industrial effluents. The intention was to assess the validity of the pretreatment under real biological conditions.

Batch mode operation was used in the reactor with activated sludge [16] starting with a solution containing *p*-NTS = 450 ppm C. Fig. 6 upper (trace shows) shows an initial spike in the DOC value after 40 min pretreatment. This is due to the increase in the carbon content of the solution when the sludge is fully mixed with the pretreated solution. After this initial mixing period the DOC values monotonically decrease up to 6 days as shown in Fig. 6. These results indicate that intermediates produced due to the photochemical pretreatment degrade less markedly after ~40 min than after 1 h pretreatment period. Therefore the biodegradability observed for our *p*-NTS pretreated solutions in Fig. 6 confirm under real field conditions the results already shown in Fig. 4a,b and Fig. 5.

The reduction in toxicity for the solution is shown next in Fig. 7. The solution used was the same as in Fig. 5. The pH during this measurements was always adjusted to pH ~7. The reduction of toxicity reflects the effect of the concentration of *p*-NTS (mg l^{-1}) and the intermediates formed during the photochemical pretreatment reducing the bacterial light emission probe as function of the pretreatment time (see Section 2). The toxicity was reduced drastically up to ~6 min. A slower decrease was subsequently observed until complete disappearance of the toxicity (~45 min). The results reported in Fig. 7 via the Microtox-test® shows the efficiency of the pretreatment applied for short time periods. The continuous decrease in the toxicity indicates that intermediates with toxic character did not develop during the photo-assisted pretreatment process.

At this point it was important to gain insight into the nature of the intermediates after the photochemical pretreatment. The results obtained are reportedly shown in Fig. 8a,b using HPLC and ILC techniques respectively.

The growth and decay of the aromatic and aliphatic intermediates is shown in Fig. 8a. Fig. 8a shows that after 5 min photochemical pretreatment the initial *p*-NTS in solution disappears. The peak in the HPLC spectrogram was followed at $\lambda = 229$ and 254 nm with a retention time of 5.9 min in the diode detector array. The scanning of this peak revealed a single aromatic component different from *p*-NTS aromatic compounds elute at longer time than aliphatic compounds. The aromatic component attained a maximum after ~5 min. It decayed afterwards within 20 min. Aliphatic compounds

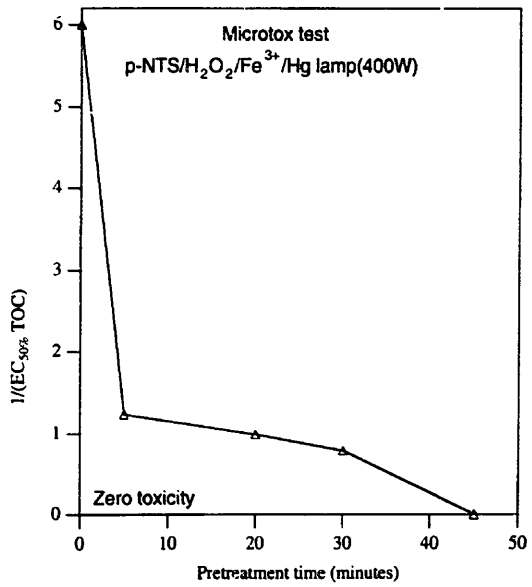

Fig. 7. Decrease in toxicity as a function of pretreatment time via the Microtox test. The solution tested had the same make up as the solution used for Fig. 5.

were detected at $\lambda = 230$ nm. A double peak was observed with a retention time of 2.5 min revealing aliphatic intermediates in solution. The analysis by HPLC was taken immediately after sampling the reactor. If not it was observed that radical reactions destroy in part the compounds to be analyzed.

In Fig. 4b, there is observed a steep increase in the BOD/TOC ratio between 30 and 40 min. Fig. 8a shows that after 30 min, *p*-NTS and recalcitrant aliphatics have been removed from the solution. Only when these two conditions are fulfilled, the ratio BOD/TOC seems to drastically increase.

As the pretreatment progresses the ·OH radical will preferentially take place on the meta position in the aromatic ring. This is the position in the ring with the least decrease in electronic density due to the nitro- and sulfate substituents withdrawing groups [10–12]

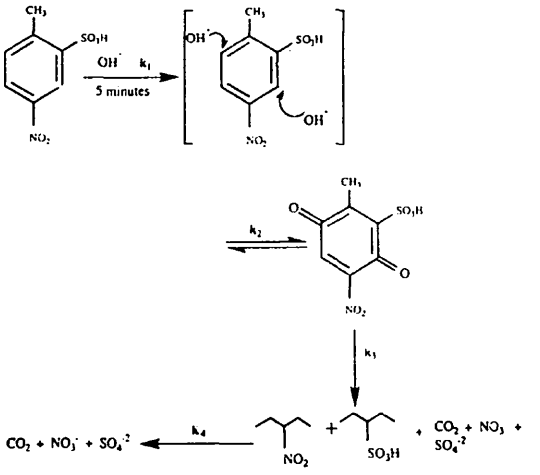

(4)

The aromatic species in Fig. 8a has been identified as belonging to benzoquinone like isomers by referencing with benzoquinone by HPLC. The scheme proposed by Eq. (4) is consistent with the degradation of substituted phenolic compounds as cited elsewhere [1,12]. The column used was the same as the one employed to measure *p*-NTS. As indicated in Eq. (4) after ca. 5 min, we are in the presence of an intermediate consisting mainly of nitro- and sulfate isomers of benzoquinone. This is not surprising since benzoquinones are the most oxidized form of quinones and will form preferentially in a medium containing H_2O_2. The type of intermediates shown above are commonly found during the chemical or biological degradation of toluene and phenol [2–7]. Smaller peaks in the HPLC spectrogram could not be identified against available commercial compounds. The ·OH radicals in solution would produce other intermediate oxidized species during this radically induced reaction. More that one degradation pathway is certainly known to take place. But since the initial reaction (k_1) is kinetically fast, the intermediates produced during these reactions could not be analyzed.

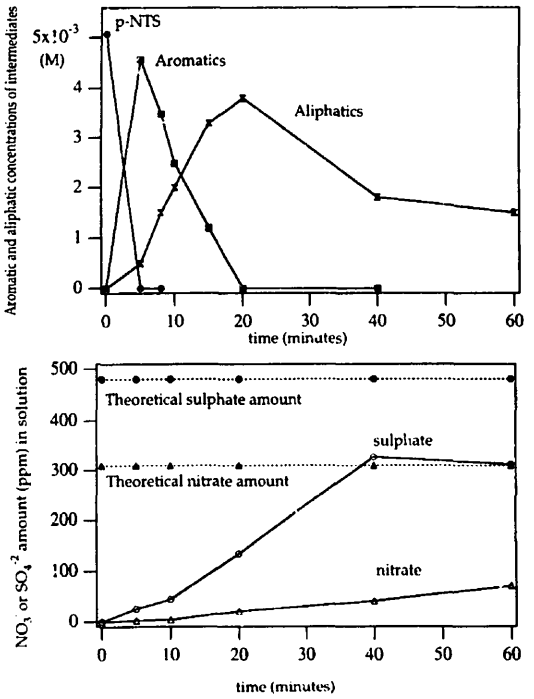

Fig. 8. (a) Aromatic and aliphatic concentration of intermediates for a solution of *p*-NTS (5×10^{-4} M), H_2O_2 (120 μl min^{-1} l^{-1}) and Fe^{+2} (130 mg l^{-1}) in a flow type reaction as a function of photochemical pretreatment time. (b) Inorganic ions found in solution as a function of photochemical pretreatment time for the solution used in Fig. 8a.

Fig. 8b shows the results for the nitrate and sulfate generation in solution as a function of photochemical pretreatment time for the same solution as used in Fig. 8a. A modest initial amount of nitrate and sulfate is generated in solution during the time of growth and decay of the aromatic species as reported previously in Fig. 8a. The rupture of the nitro- and sulfate bond take place from aliphatic moieties but remain under the stoichiometric amount up to 1 h.

3.3. Dynamics and efficiencies of the coupling of the biological and photochemical stages

Fig. 9 shows the flow parameters in a loop system for the coupled reactor presented in Fig. 1 at two different flow rates. The H_2O_2 was added to the photoreactor at the rate of 0.12 ml min^{-1}. A recirculation rate of 24 l h^{-1} was used to degrade the initial solution of *p*-NTS = 420 mg C l^{-1} (5.4×10^{-3} M at pH = 2.7) into aliphatic intermediates. Applying a feeding rate of 15 ml min^{-1} as shown in Fig. 9a, the concentration of *p*-NTS attained zero using 2.9×10^{-3} H_2O_2 moles l^{-1} h^{-1}. The degradation rate of 222 mg C l^{-1} h^{-1} observed in the

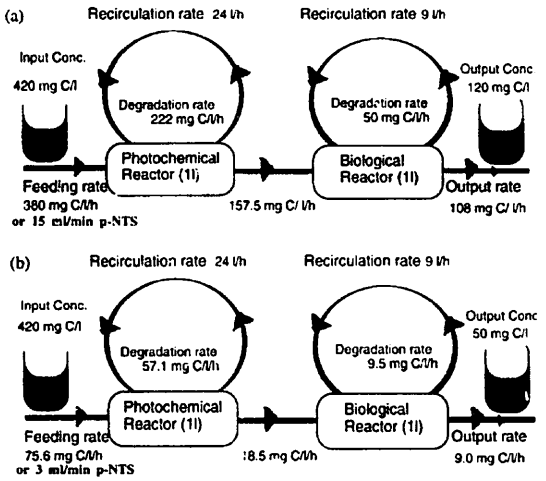

Fig. 9. Flow diagram for the combined reactor used in the photochemical–biological degradation of *p*-NTS.

photoreactor required 70 10^{-3} moles l^{-1} h^{-1} of H_2O_2. The aromatic groups disappear in the photoreactor (as seen by HPLC) before coupling of the solution with the bioreactor is put in place in Fig. 9a. Dissolved O_2 from the Fenton pretreatment was seen to be useful during the ensuing biological degradation. There was no need to eliminate the residual H_2O_2 used during the pretreatment since the conditions were found to completely react this oxidant in the first step. The Merckoquant®-test was used for this determination as mentioned previously in Section 2. In this way the addition of catalase [14] or sodium sulfite [15] to eliminate the residual H_2O_2 was avoided as used in recent studies involving coupled reactors.

Adapted bacteria from BOD_5 experiments were fixed on biolite in the column of the biological reactor. The adapted bacteria in the bioreactor evolves naturally in the system over 3–4 weeks. The aliphatic intermediates leaving the photoreactor as shown in Fig. 8a is the only carbon source entering the bioreactor. During the biodegradation automated regulation of the pH to a value ~7 in the bioreactor was maintained by means of a Bioengineering control unit. The high recirculation rate of 9 l h^{-1} allowed mixing in the bioreactor producing optimal contact between the biolite and the solution used. The relatively high value of 120 mg C l^{-1} (Fig. 9a) for the leftover carbon content after biological treatment could be further decreased. This was possible using a batch mode operation in the bioreactor. This operation mode allowed to work over longer reaction periods with increased carbon abatement in the biological stage. The overall low degradation rate in the bioreactor is due to: (a) the relatively short bioreactor residence time; (b) the relatively high flow rate used of 15 ml min^{-1}; (c) the well known slow bacterial action of non-adapted bacterial strains; and (d) the persistence in the solution of nitro- and sulfate-aliphatic chains. The latter compounds have been reported to be less biodegradable than non-substituted short chain aliphatic compounds [12].

When the overall flow rate was decreased in the coupled reactor, the output rate was seen to be more favorable in terms of the C-content in the effluent solution. This is due to the longer residence times of the *p*-NTS solution in the coupled reactor. In effect, Fig. 9b shows an output rate of only 9 mg C l^{-1} h^{-1} a more favorable value than the corresponding value reported in Fig. 9a.

The reactor efficiency calculated in terms of *p*-NTS removal during the degradation is unity since it is fully degraded in the photochemical reactor in very short times as followed by HPLC measurements. The efficiency for the photochemical, the biological and the overall degradation in terms of TOC could be estimated according to Scott and Ollis [1] based on the expression:

$$\text{eff photo} = \frac{\text{Initial TOC } p-\text{NTS} - (\text{TOC } p\text{-NTS after photoreactor} + \text{TOC interm leaving photoreactor})}{\text{initial TOC } p-\text{NTS}} \quad (5)$$

$$\text{eff biol} = \frac{\text{TOC interm leaving photoreactor} - \text{TOC interm leaving bioreactor}}{\text{TOC intermediates leaving photoreactor}} \quad (6)$$

$$\text{eff overall} = \frac{\text{initial TOC } p-\text{NTS} - \text{TOC interm leaving bioreactor}}{\text{initial TOC } p-\text{NTS}} \quad (7)$$

Substituting the numerical values in Eqs. (5)–(7) from Fig. 9a and knowing that no *p*-NTS leaves the photoreactor a degradation of ~63% can be estimated for the photochemical stage. The efficiency for the biological stage estimated according to Eq. (6) is ~31%. The overall efficiency (Eq. (7)) was seen to be 71%. If 30 ppm C was due to physiological bacterial carbon then the efficiency in the bioreactor could be estimated as 78%. Fig. 9b shows the results of experiments when the flow rate used as of 3 ml min^{-1} or 0.18 (l h^{-1}) which allows for a longer contact time during reaction operation. The values for the efficiencies for the cycle presented in Fig. 9b have been already mentioned in the abstract.

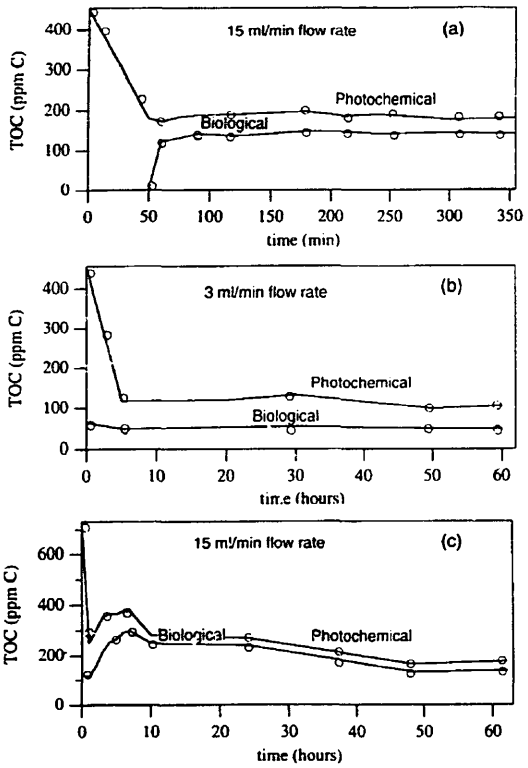

Fig. 10. (a,b) TOC decrease due to the coupled flow reactor for a *p*-NTS solution as a function of flow rate and (c) for solution with a higher C-content higher than in (a).

3.4. Effect of the residence times on the biological degradation

Fig. 10 shows the reduction in the coupled photochemical–biological system under continuous operation as shown by Fig. 9. Fig. 10a shows an initial reduction of TOC from 450 ppm C to ~ 185 ppm C within 50 min. A 15 ml min^{-1} (0.9 l h^{-1}) flow rate is applied equivalent to a residence time of 1.1 h in the photoreactor. The subsequent reduction of carbon content in the bioreactor was observed to reach TOC = 130 ppm C. In Fig. 10b the equalized flow rate was decreased to 3 ml min^{-1} or an equivalent residence time of 5.5 h. A more favorable reduction of the carbon content of about 120 ppm C entering the bioreactor was observed. A reduction from about 120 to 60 ppm C takes place in the bioreactor under this flow. Fig. 10c reports the results when the TOC content of the initial solution was increased to 700 ppm C. When the initial TOC was decreased by a factor of three in the photochemical stage, further reduction of the C-content in the bioreactor was modest. This was expected due to the more difficult bacterial degradation on solutions with a higher carbon content. The reaction intermediates are possibly different in nature when a higher load is applied. This would account for the lower efficiencies observed in the bioreactor for concentrated solutions. The reduction in the carbon content as a function of the initial concentration of the pollutant and the flow rate used were not proportionally related as shown by the results in Fig. 10.

4. Conclusions

This study demonstrates the useful photo-Fenton pretreatment of an aromatic (*p*-NTS) prior to biotreatment with a tandem reactor concept. The main parameters affecting the performance of the photo-assisted reactor have been reported in this study. The first stage in the reactor was affected by the amount of substrate, oxidant and the flow rate used. During the pretreatment the *p*-NTS removal efficiency was related to the minimum irradiation time to use for the shortest possible time the expensive photons. This study concentrated on Fenton treatment under illumination since dark reactions using the Fenton reagent were shown to be slow and inefficient. The fixed biomass in the bioreactor resisted the variations of substrate concentrations and flow rate over long periods (up to 2 months). The reactor could be operated within this period from a low (40 ppm C) up to a high concentration of substrate of ~ 1000 ppm C without altering the overall performance of the system. Biolite was a cheap support and allowed an adequate contact during the recirculation in the bioreactor. No appreciably increase in the biomass volume was observed during operation within a period of a week. Toxic intermediate products did not develop during degradation in the solution as revealed by toxicity test. In spite of the initial photoreactor treatment and beneficial reduction of C in the biological second stage no full mineralization was observed. It seems that one part of the C intermediates degrades easily, but another part even lacking aromatic character does not undergo easily biodegradation in the second stage. Fixed biomass bioreactors take up to ten times less space than more conventional reactors using suspended biomass [12]. Land in Switzerland is expensive and hardly available and therefore studies in this direction are warranted.

Acknowledgements

The skillful technical assistance of J-P Kradolfer is duly appreciated. This work was supported by grant No. EV5V-CT93-0249 from the Commission of European Communities (OFES Contract No. 950 031, Bern) and INTAS Cooperation Project Brussels No. 094-642.

References

[1] P.J. Scott, D.F. Ollis, Environ. Progr. 14 (1995) 88.
[2] G. Helz, R. Zepp, D. Crosby, Aquatic and Surface Chemistry, Lewis Publ., Boca Raton, FL, 1994.

[3] L. Minsker, C. Pulgarin, P. Peringer, J. Kiwi, New J. Chem. 18 (1994) 793.
[4] Ch. Seignez, C. Pulgarin, S. Bosco, P. Peringer, J. Bandara, J. Kiwi, Proceedings World Environmental Congress, London, Ont., Canada, 1995, p. 243.
[5] H. Stockinger, Dissertation, No. 11063, Zurich, 1995.
[6] F. Geiger, Biotechnol. Progr. 8 (1995) 67.
[7] C. Pulgarin, J. Kiwi, Langmuir 11 (1995) 519.
[8] Ch. Seignez, V. Mottier, C. Pulgarin, N. Adler, P. Peringer, Environ. Progr. 128 (1993) 306.
[9] M. Bokhamy, N. Adler, C. Pulgarin, M. Deront, Ch. Seignez, P. Peringer, Appl. Microb. Biotechnol. 41 (1994) 110.
[10] J. Kiwi, C. Pulgarin, P. Peringer, M. Grätzel, New J. Chem. 17 (1993) 487.
[11] J. Bolton, K. Bircher, W. Tumas, Ch. Tolman, Adv. Oxid. Technol. 1 (1996) 13.
[12] F. Pitter, J. Chudoba, Biodegradability of Organic Substances in the Aquatic Environment, CRC Press, Boca Raton, FL, 1990.
[13] D. Vasseur, M. Cook, T. Leisinger, Appl. Environ. Microb. 17 (1986) 153.
[14] P. Bowers, W. Gaddipati, Water Sci. Tech. 21 (1989) 477.
[15] A. Adams, A.N. Scanlon, N. Secrist, Environ. Sci. Technol. 28 (1994) 1812.
[16] OECD Guidelines for Testing of Chemicals, Reg 392 B, 1981.